

Alkali Metal Complexes of a Bis(diphenylphosphino)methane Functionalized Amidinate Ligand: Synthesis and Luminescence

Christina Zovko,^[a] Christoph Schoo,^[a] Thomas J. Feuerstein,^[a] Luca Münzfeld,^[a] Nicolai D. Knöfel,^[a] Sergei Lebedkin,^[b] Manfred M. Kappes,^[b, c] and Peter W. Roesky*^[a]

In memoriam of Prof. Markus Gerhards.

Abstract: A novel bis(diphenylphosphino)methane (DPPM) functionalized amidine ligand (DPPM–C(N-Dipp)₂H) (Dipp = 2,6-diisopropylphenyl) was synthesized. Subsequent deprotonation with suitable alkali metal bases resulted in the corresponding complexes [M{DPPM–C(N-Dipp)₂}(L_n)] (M = Li, Na, K, Rb, Cs; L = thf, Et₂O). The alkali metal complexes form monomeric species in the solid state, exhibiting intramolecular metal- π -interactions. In addition, a caesium derivative [Cs{PPh₂CH₂-C(N-Dipp)₂}]₆ was obtained by cleavage of a diphenylphosphino moiety, forming an unusual six-membered ring structure in the solid state. All complexes were fully

characterized by single crystal X-ray diffraction, NMR spectroscopy, IR spectroscopy as well as elemental analysis. Furthermore, the photoluminescent properties of the complexes were thoroughly investigated, revealing differences in emission with regards to the respective alkali metal. Interestingly, the hexanuclear [Cs{PPh₂CH₂-C(N-Dipp)₂}]₆ metallocycle exhibits a blue emission in the solid state, which is significantly red-shifted at low temperatures. The bifunctional design of the ligand, featuring orthogonal donor atoms (N vs. P) and a high steric demand, is highly promising for the construction of advanced metal and main group complexes.

Introduction

Amidates are N-chelating ligands of the general form [RC(NR')₂]⁻ and represent one of the most common ligand systems in coordination chemistry.^[1–2] They are accessible via various synthetic routes and can be easily modified by varying the substituents (R, R') of the heteroallylic NCN moiety. This allows

customization of the ligand in terms of steric demand and electronic properties as well as the introduction of additional functionalities. Hence, amidates are widely used in the formation and stabilization of complexes, ranging from main group elements to transition and f-block metals.^[3–8] In general, monoanionic amidates provide a mono- or bidentate support for metal ions, yet the introduction of additional heteroatom donor sites into the amidate scaffold allows for extension to advanced coordination motifs as well as the potential formation of heteromultimetallic complexes.^[9] In recent years, P,N-type ligands, possessing both nitrogen and phosphorus donor sites, have been proven particularly suitable for this task (Figure 1).^[10–11] For instance, the synthesis of different amidate ligands with attached phosphine moieties has been reported in literature (Figure 1c), which were subsequently used to prepare main group and transition metal compounds.^[12–13] In this context, the composition and design of a multidentate P,N-ligand, for example the proximity of functional units or the steric demand, play a decisive role in promoting specific arrangements and metal-metal interactions.^[14] This fine-tuning allows customizing the properties and applications of the corresponding organometallic material in terms of photophysical and catalytic properties.^[15–16] For the synthesis of a novel, multidentate P,N-ligand, the integration of a bis(diphenylphosphino)methane (DPPM) functionality into an amidate system seemed to be advantageous, utilizing the different properties of hard amidate and soft phosphine donor centers.^[17–18] In general, DPPM and its derivatives are well-established ligand systems in coordination chemistry that

[a] C. Zovko, Dr. C. Schoo, Dr. T. J. Feuerstein, L. Münzfeld, Dr. N. D. Knöfel, Prof. Dr. P. W. Roesky
Institute of Inorganic Chemistry
Karlsruhe Institute of Technology (KIT)
Engesserstraße 15, 76131 Karlsruhe (Germany)
E-mail: roesky@kit.edu

[b] Dr. S. Lebedkin, Prof. Dr. M. M. Kappes
Institute of Nanotechnology
Karlsruhe Institute of Technology (KIT)
Hermann-von-Helmholtz-Platz 1, 76344, Eggenstein-Leopoldshafen (Germany)

[c] Prof. Dr. M. M. Kappes
Institute of Physical Chemistry
Karlsruhe Institute of Technology (KIT)
Fritz-Haber-Weg. 2, 76131 Karlsruhe, Germany

Supporting information for this article is available on the WWW under <https://doi.org/10.1002/chem.202102243>

This manuscript is part of a Special Issue "Cooperative effects in heterometallic complexes".

© 2021 The Authors. Chemistry - A European Journal published by Wiley-VCH GmbH. This is an open access article under the terms of the Creative Commons Attribution Non-Commercial License, which permits use, distribution and reproduction in any medium, provided the original work is properly cited and is not used for commercial purposes.

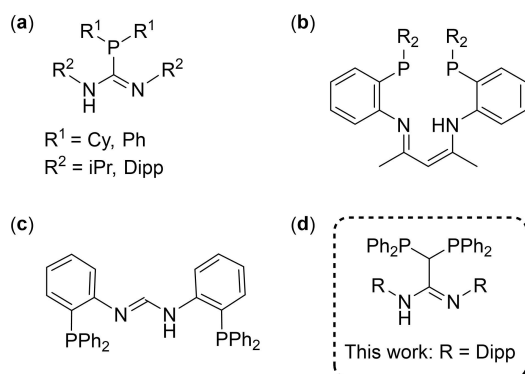


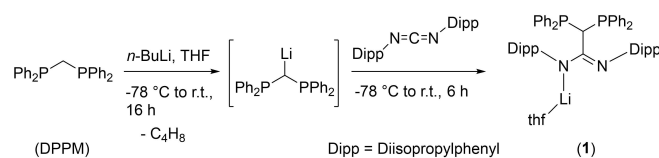
Figure 1. A series of phosphine-functionalized N-donor ligand systems, applicable for the construction of metal complexes: (a) phosphorus guanidine,^[11,21–22] (b) β -diketimine,^[10] (c)^[12] and (d) amidines. The introduction of additional phosphorus containing moieties into the respective ligand scaffold enables the formation of specific pockets and coordination motifs.

enable bidentate chelating and bridging coordination modes of suitable metal ions.^[19] In 2012, a DPPM-functionalized carboxylate, which can be considered as oxygen analogues of the amidinate anions, was described by Duchateau et al. and successfully applied for the synthesis of metal complexes.^[20] Following on from this, the extension to a corresponding amidinate ligand system enables the introduction of additional side groups and functionalities and thus the construction of advanced coordination pockets and motifs.

To the best of our knowledge, a DPPM-functionalized amidine system (Figure 1d), exhibiting a multidentate P_2N_2 -type coordination sphere, as described herein, has not yet been reported. The bifunctional ligand exhibits orthogonal, opposing functionalities that allow for multiple coordination modes. These properties render it highly interesting for the synthesis of metal and main group complexes in addition to heterometallic structures. Furthermore, we report on the synthesis of the ligand's alkali metal complexes $[M\{DPPM-C(N-Dipp)_2\}(L)_n]$ ($M = \text{Li, Na, K, Rb, Cs}$; $L = \text{thf, Et}_2\text{O}$) as well as the remarkable caesium derivative $[Cs\{PPh_2CH_2-C(N-Dipp)_2\}]$, which forms an unusual six-membered ring structure in the solid state. Investigation of the photoluminescence (PL) properties in the solid state revealed interesting PL behavior for the respective alkali metal complexes.

Results and Discussion

The bis(diphenylphosphino)methane (DPPM) functionalized amidinate ligand was obtained by a two-step synthesis route on a multigram scale (Scheme 1). First, DPPM was reacted with *n*-BuLi, leading to deprotonation of the methylene moiety. Subsequently, bis(2,6-diisopropylphenyl)carbodiimide was added to the reaction mixture to obtain the lithium salt of the DPPM-functionalized amidinate $[Li\{DPPM-C(N-Dipp)_2\}(\text{thf})]$ ($\text{thf} = \text{tetrahydrofuran}$, $\text{Dipp} = 2,6\text{-diisopropylphenyl}$) (**1**) via a nucleophilic C–C coupling reaction. The Dipp-functionalized carbodiimide was selected to introduce sterically demanding



Scheme 1. Synthesis of DPPM-functionalized amidinate ligand **1** via a two-step reaction.

substituents to the ligand. The introduction of other substituents can be easily accomplished by selecting other suitable carbodiimides.

Single crystals of **1**, suitable for X-ray analysis, were obtained by slow diffusion of *n*-pentane into a THF solution. A crystallization process is necessary to purify the compound by separation of unreacted DPPM. Compound **1** crystallizes in the triclinic space group $P\bar{1}$ with one molecule in the asymmetric unit. The molecular structure of **1** in the solid state, as shown in Figure 2, reveals the expected bisphosphine-functionalized amidinate structure. Here, the lithium ion is κ^1 -coordinated by one of the nitrogen atoms of the amidinate moiety. The monodentate metal coordination mode is regularly observed for amidinates with sterically demanding substituents.^[1] Similarly, a dimerization process, which is not uncommon for lithium amidinates, is prohibited, leading to the formation of a monomeric species in the solid state. The coordination sphere of the lithium ion is further saturated by an intramolecular π -arene interaction and an additional THF molecule. In general, bulky *N*-bound aryl substituents of amidinates can adopt a *syn*- or *anti*-configuration. This has a great influence on the ligand's coordination behavior, as an *anti*-configuration supports a coordination mode in which the metal ion is coordinated to a nitrogen atom of the NCN moiety and the π -arene system.^[23] Accordingly, the metal π -arene interaction in **1** is enabled by

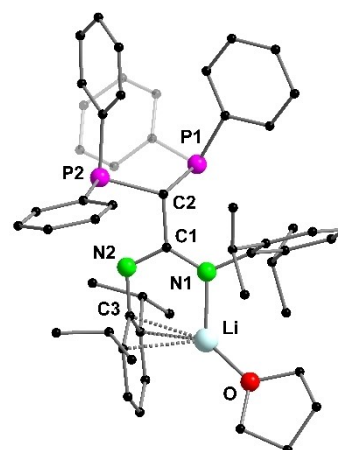
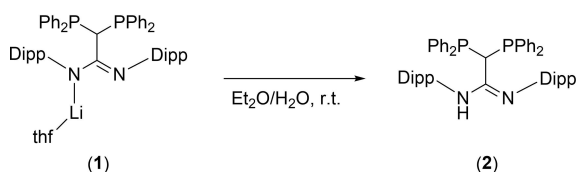


Figure 2. Molecular structure of **1** in the solid state. Hydrogen atoms are omitted for clarity. Selected bond lengths [\AA] and angles [$^\circ$]: N1–Li 1.951(3), P1–C2 1.898(2), P2–C2 1.878(2), N1–C1 1.342(2), N2–C1 1.314(2), N2–C3 1.410(2), C1–C2 1.537(2), Li–O 1.882(3), Li–C3 2.347(4); P1–C2–P2 116.79(8), N1–C1–N2 122.50(13), N1–C1–C2 123.32(14), N2–C1–C2 114.17(13), C1–N1–Li 120.00(14), C1–N2–C3 114.57(13).

anti-configuration of the aromatic Dipp groups, as a consequence of the DPPM moiety's high steric demand on the amidinate backbone. The lithium ion is η^3 -coordinated with relatively short contacts to the *ipso* and *ortho* carbon atoms of one of the Dipp substituents. (Li–C distances of 2.347(4), 2.434(4) and 2.650(4) Å). The structural motif and bond lengths are in agreement with the comparable lithium amidinate [Li{(Dipp-N)₂C-tBu}(thf)].^[23] The angle of the NCN unit (N1-C1-N2 122.50(13)°) is within the usual range for an amidinate system (in comparison, the NCN angle of lithium Dipp-formamidinate is 120.0(2)°).^[24] The corresponding angle of the DPPM moiety (P1-C2-P2) is 116.79(8)°, which is slightly widened in comparison to the starting material bis(diphenylphosphino)methane (107.63(10)°).^[25] The C–N bond distances of the amidinate moiety are slightly different (N1–C1 1.342(2) Å, N2–C1 1.314(2) Å), indicating a rather localized charge distribution of the NCN unit.

Furthermore, compound **1** was analyzed by NMR and IR spectroscopy as well as elemental analysis. In the ³¹P{¹H} NMR spectrum (C₆D₆) a single resonance is detected at $\delta = -3.2$ ppm, indicating a symmetrical behavior of the diphenylphosphino moiety in solution. The resonance is significantly downfield shifted compared to DPPM ($\delta = -22.0$ ppm).^[26] In the corresponding ¹H and ¹³C{¹H} NMR spectra of **1**, a single set of resonances is observed for the ligand system, pointing to the symmetric behavior of compound **1** in solution. A characteristic triplet ¹³C{¹H} resonance for the amidinate unit (NCN) is detected at $\delta = 164.7$ ppm (²J_{C,P} = 13.4 Hz), whereas a triplet resonance for the DPPM-CH moiety is observed at $\delta = 38.3$ ppm (¹J_{C,P} = 40.5 Hz). Moreover, a single resonance at $\delta = -1.6$ ppm is observed in the ⁷Li NMR spectrum of **1**, which is in agreement with other lithium amidinates and indicates a monomeric species in solution.^[27–28]

Secondly, [Li{DPPM–C(N–Dipp)₂}(thf)] (**1**) was quenched by addition of H₂O to a diethyl ether solution of the compound to obtain the respective DPPM-amidine **2** (Scheme 2). Colorless single crystals of **2**, suitable for X-ray analysis, were obtained by slow evaporation of an Et₂O solution. Compound **2** crystallizes solvent-free in the monoclinic space group *P2₁/n* with two molecules in the asymmetric unit (Figure 3). The NCN (122.6(2)°) angle of compound **2** is in a similar range as that of compound **1** as well as related amidines such as *N,N'*-bis(2,6-diisopropylphenyl)formamidine (123.3(2)°).^[29] In accordance with **1**, the NCN unit of **2** is not delocalized, as can be observed from the different C–N bond lengths (N1–C1 1.365(2) Å; N2–C1 1.295(2) Å).



Scheme 2. Synthesis of the amidine **2** by protonation of the corresponding lithium amidinate **1**.

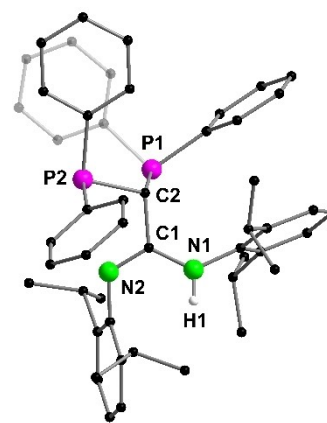
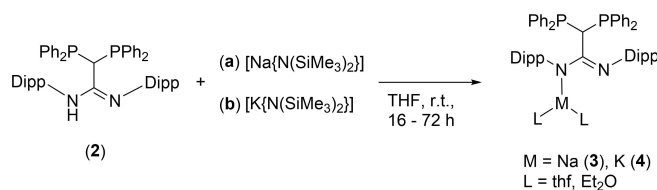


Figure 3. Molecular structure of **2** in the solid state. Carbon-bound hydrogen atoms are omitted for clarity. The asymmetric unit contains two independent molecules, only one of which is shown in the figure, since the respective bond lengths and angles are similar. Selected bond lengths [Å] and angles [°]: P1–C2 1.905(2), P2–C2 1.886(2), N1–C1 1.365(2), N2–C1 1.295(2), C1–C2 1.513(2); P1–C2–P2 112.50(9), N1–C1–N2 122.6(2), N1–C1–C2 119.9(2), N2–C1–C2 117.3(2).

The formation of a dimeric structure via H-bonds, as reported for *N,N'*-bis(2,6-diisopropylphenyl)-formamidine,^[29] cannot be observed in the solid state, probably due to the high steric influence of the DPPM moiety and the Dipp groups, which again adopt an *anti*-configuration. The ¹H NMR spectrum (C₆D₆) of **2** confirms the presence of a NH proton detected at $\delta = 5.96$ ppm, indicating complete protonation of the ligand. The corresponding ³¹P{¹H} NMR spectrum shows a single resonance at $\delta = -5.2$ ppm, which is slightly shifted upfield compared to compound **1**.

Subsequently, deprotonation of the amidine ligand **2** with alkali metal bases [M{N(SiMe₃)₂}] (M = Na, K) led to the compounds [M{DPPM–C(N–Dipp)₂}(L)₂] (M = Na (**3**), K (**4**) and L = thf, Et₂O) (Scheme 3). Interestingly, the use of other common alkali metal precursors such as NaH, KH, or elemental Na and K led to decomposition of the ligand system.

Single crystals of **3** and **4** were obtained by slow diffusion of *n*-pentane into a THF solution of the respective compound, resulting in the formation of the corresponding THF adducts. For potassium complex **4** single crystals were also obtained by slow evaporation of diethyl ether, which led to the coordination of Et₂O accordingly. In this work, only the respective Et₂O structure of **4** is discussed in detail. Compounds **3** and **4** are isostructural (neglecting different solvent coordination) and



Scheme 3. Synthesis of alkali amidinates **3** and **4** by reaction of DPPM-amidine **2** and [M{N(SiMe₃)₂}] (M = Na, K).

both crystallize in the triclinic space group $P\bar{1}$ with one molecule in the asymmetric unit. In the case of **3**, two thf molecules are coordinated to the sodium atom (Figure 4, left). Similarly, the potassium atom of compound **4** is coordinated by two diethyl ether molecules (Figure 4, right), as a result of the different crystallization processes. Analogous to **1**, the sodium and potassium ions are κ^1 -coordinated by the NCN moiety and their coordination sphere is additionally saturated by intramolecular metal π -arene interactions, which are enabled due to an *anti*-configuration of the Dipp substituents. In case of sodium complex **3**, η^3 -coordination to one of the Dipp groups is observed analogous to lithium amidinate **1** (Na–C: 2.815(2)–3.115(2) Å). The larger ionic radius of potassium in complex **4** results in a η^6 - π -arene interaction, with K–C distances in the range of K–C3 3.0906(14) to K–C6 3.342(2) Å. This is in agreement with the comparable potassium amidinates [K{(Dipp-N)₂C–Ph}(thf)₃] and [K{(Dipp-N)₂C–tBu}(thf)₃], which also exhibit η^6 - π -arene interactions.^[23] The respective NCN and PCP angles of **3** and **4** differ only insignificantly from **1**, which therefore appear independent of the coordination of different alkali metals.

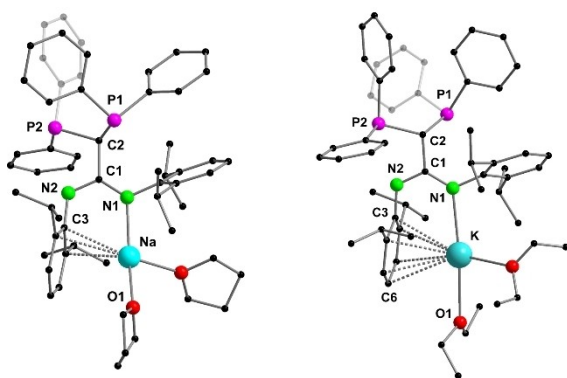
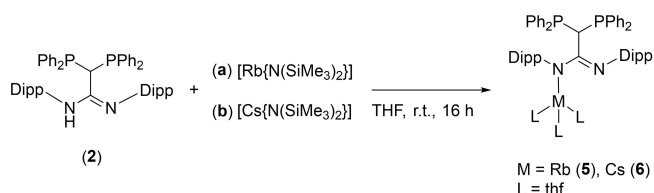


Figure 4. Molecular structure of **3** (left) and **4** (right) in the solid state. Hydrogen atoms are omitted for clarity. Selected bond lengths [Å] and angles [°] for **3**: N1–Na 2.374(2), P1–C2 1.905(2), P2–C2 1.877(2), N1–C1 1.339(2), N2–C1 1.313(2), N2–C3 1.407(2), C1–C2 1.543(2), Na–O1 2.359(2), Na–C3 2.815(2); P1–C2–P2 115.60(8), N1–C1–N2 123.43(14), N1–C1–C2 123.41(13), N2–C1–C2 113.09(14), C1–N2–C3 118.50(13), C1–N1–Na 125.45(10). Selected bond lengths [Å] and angles [°] for **4**: N1–K 2.7879(11), P1–C2 1.8970(14), P2–C2 1.8784(14), N1–C1 1.334(2), N2–C1 1.320(2), C1–C2 1.544(2), K–O1 2.8499(12), K–C3 3.0906(14), K–C6 3.342(2); P1–C2–P2 116.64(7), N1–C1–N2 123.71(12), N1–C1–C2 124.20(12), N2–C1–C2 112.07(11), C1–N2–C3 119.03(11), C1–N1–K 126.30(9).



Scheme 4. Synthesis of rubidium and caesium amidinates **5** and **6** by reaction of DPPM-amidinate **2** with [Rb{N(SiMe₃)₂}] and [Cs{N(SiMe₃)₂}], respectively. For **6**, the coordination of three solvent molecules is assumed, however this was not confirmed by XRD measurements.

Compounds **3** and **4** were also analyzed by NMR spectroscopy, IR spectroscopy and elemental analysis. The ³¹P{¹H} NMR spectra (C₆D₆) of **3** and **4** depict a single resonance at $\delta = -3.3$ ppm (**3**) and $\delta = -1.7$ ppm (**4**), which are in the same range as lithium compound **1** ($\delta = -3.2$ ppm). In the respective ¹H and ¹³C{¹H} NMR spectra a similar set of resonances is detected as for **1**, but the resonances for potassium compound **4** appear comparatively broader.

To complete the series of alkali metals, the corresponding rubidium and caesium amidinates [Rb{DPPM–C(N–Dipp)₂}(thf)₃] (**5**) and [Cs{DPPM–C(N–Dipp)₂}(thf)₃] (**6**) were synthesized, following the methodology that facilitated the reaction of **3** and **4** (Scheme 4).

In case of the rubidium complex **5**, colorless single crystals were obtained by slow diffusion of *n*-pentane into a THF solution. Compound **5** crystallizes in the monoclinic space group $P2_1/c$ with one molecule in the asymmetric unit. As expected, the molecular structure of **5** in the solid state, shown in Figure 5, is almost identical to the other alkali amidinates **1**, **3** and **4**. The coordination sphere of the rubidium ion is saturated by a η^6 - π -arene interaction with one of the Dipp substituents as observed for potassium complex **4**. Due to the enhanced size of the rubidium cation three THF molecules additionally coordinate to the metal center. Despite the larger ionic radius of rubidium, the NCN angle of **5** is very similar to the other alkali amidinates (range between 122.43(14)° and 125.6(2)°). As expected, the N–M (M = Li, Na, K, Rb) bond lengths increase with increasing metal ion radius from 1.951(3) Å (**1**), 2.374(2) Å (**3**), 2.7879(12) Å (**4**) to 2.973(2) Å (**5**).

The corresponding caesium complex [Cs{DPPM–C(N–Dipp)₂}(thf)₃] (**6**) was crystallized by slow diffusion of *n*-pentane into a THF solution. However, no single crystals of **6**, suitable for X-ray analysis, were obtained. Nevertheless, a structure analogous to the other alkali metal complexes is assumed, with at least three thf molecules coordinated to the caesium ion. This was confirmed by NMR spectroscopy, among other methods. In

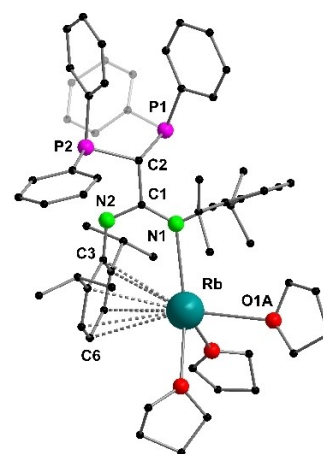
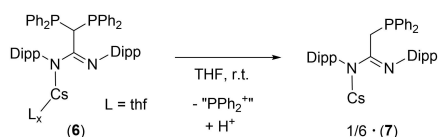


Figure 5. Molecular structure of **5** in the solid state. Hydrogen atoms are omitted for clarity. Selected bond lengths [Å] and angles [°]: N1–Rb 2.973(2), P1–C2 1.893(2), P2–C2 1.873(2), N1–C1 1.333(3), N2–C1 1.317(3), C1–C2 1.548(3), Rb–C3 3.289(2); P1–C2–P2 115.66(12), N1–C1–N2 125.6(2), N1–C1–C2 122.3(2), N2–C1–C2 112.0(2), C1–N2–C3 121.2(2), C1–N1–Rb 125.02(14).

the $^{31}\text{P}\{^1\text{H}\}$ NMR spectra (THF- d_6) of **5** and **6** a single resonance is detected at $\delta=0.0$ ppm (**5**) and $\delta=0.6$ ppm (**6**), respectively, which are slightly shifted downfield compared to the other alkali metal complexes. As observed for potassium complex **4**, relatively broad resonances are detected in the ^1H and $^{13}\text{C}\{^1\text{H}\}$ NMR spectra of **5** and **6** (at 298 K), hence the resonance resolution seems to decrease along with the size of the alkali metal cation. This likely results from dynamic processes in solution, thus ^1H and $^{13}\text{C}\{^1\text{H}\}$ NMR spectra were also recorded at lower temperatures (down to 233 K; see Figure S24 and S28), which significantly amplified resonance resolution. In addition, the IR spectra of both compounds **5** and **6** are almost identical, confirming the isostructural composition of the two complexes.

During the synthesis of **6**, NMR spectroscopy indicated a decomposition of $[\text{Cs}\{\text{DPPM}-\text{C}(\text{N-Dipp})_2\}(\text{thf})_x]$ over time, a process that seems to be enhanced by application of an excess of $[\text{Cs}\{\text{N}(\text{SiMe}_3)_2\}]$. In the process, one of the $\{\text{PPh}_2\}$ groups of the DPPM moiety is cleaved off and replaced by a hydrogen atom, resulting in the formation of monophosphine-functionalized amidinate $[\text{Cs}-\text{PPh}_2\text{CH}_2-\text{C}(\text{N-Dipp})_2]_6$ (**7**) (Scheme 5). Although P-C bond cleavages are known for DPPM and its derivatives,^[30–33] the mechanism of the reaction is unclear in our case. When monitoring the decomposition of **6** by $^{31}\text{P}\{^1\text{H}\}$ NMR



Scheme 5. Formation of caesium complex **7** by decomposition of **6** over time. One of the $\{\text{PPh}_2\}$ moieties per molecule is cleaved off in the process to give $[\text{Cs}-\text{PPh}_2\text{CH}_2-\text{C}(\text{N-Dipp})_2]_6$ (**7**), which forms a six-membered ring structure in the solid state. Merely the respective monomer unit of **7** is shown in the scheme, which is considered to be present in solution.

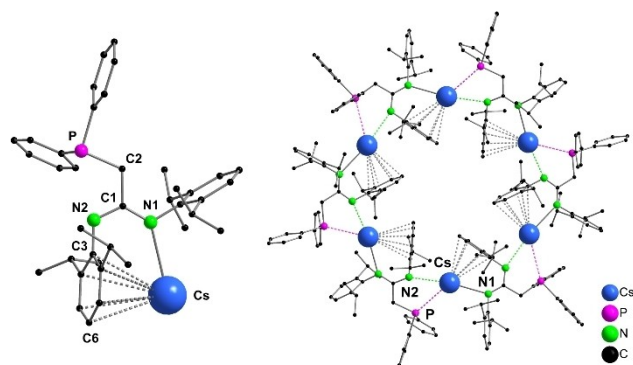


Figure 6. Molecular structure of **7** in the solid state. Hydrogen atoms and solvent molecules (THF, *n*-pentane) are omitted for clarity. Selected bond lengths [Å] and angles [°]: N1-Cs 3.069(2), P-C2 1.843(3), N1-C1 1.324(3), N2-C1 1.327(4), C1-C2 1.520(3), N2-C3 1.411(3), Cs-C3 3.573(2), Cs-C6 3.591(3); N1-C1-N2 125.2(2), N1-C1-C2 120.5(2), N2-C1-C2 114.3(2), C1-C2-P 114.1(2), C1-N1-Cs 133.3(2), C1-N2-C3 117.5(2). The asymmetric unit is displayed on the left side. Right side: Molecular structure of **7** in the solid state, displaying formation of a six-membered ring structure $[\text{Cs}-\text{PPh}_2\text{CH}_2-\text{C}(\text{N-Dipp})_2]_6$ due to intermolecular interactions between Cs-N2 (green, dotted), Cs-P (pink, dotted) and Cs- π -interactions. Respective atom distances [Å] and angles [°]: P-Cs 3.7753(9), Cs-N2 3.188(2); N1-Cs-N2 171.08(5).

spectroscopy, a degradation of **6** is monitored and small signals of **7** can be observed after only a few hours (Supporting Information, Figure S32). After one week, a mixture of species was visible, yet only **7** was identified as one of the products, which was isolated in a crystalline yield of about 40%.

Single crystals of **7** were readily obtained by slow diffusion of *n*-pentane into a THF solution. Compound **7** crystallizes in the trigonal space group *R*-3 with one molecule, as part of a six-membered ring structure, in the asymmetric unit (Figure 6). The molecular structure of **7** in the solid state confirms the cleavage of one $\{\text{PPh}_2\}$ moiety per molecule. The hexanuclear ring structure is formed via intermolecular interactions between caesium and the nitrogen atom of an adjacent NCN unit with a Cs-N2 distance of 3.182(3) Å (in comparison: Cs-N1 3.066(3) Å) as well as Cs- η^6 - π interactions (Cs-C distances: 3.573(2) to 3.636(3) Å). In addition, each phosphine moiety orientates to an adjacent caesium ion (Cs-P 3.7753(9) Å), favored by the soft character of the caesium cation and the flexible alignment of the CH_2PPh_2 units, possibly contributing to the stabilization of the ring structure.

The Cs-P distance of 3.7753(9) Å is slightly longer than previously reported Cs-P contacts, for example in comparable Cs phosphide or phosphinomethanide complexes (Cs-P separations of 3.52–3.64 Å).^[34–37] Organometallic caesium complexes have a tendency to form coordination oligomers and polymers in the solid state, such as infinite chains or three-dimensional networks,^[38–42] featuring unique coordination motifs. This characteristic, amongst others, is often caused by intermolecular caesium- π -arene interactions. However, merely two hexanuclear caesium rings are reported in literature, utilizing either a bis(iminophosphorano)-methanide or a *m*-terphenyl cyclopentadienyl ligand as a scaffold.^[43–44] In both cases the ring structure is stabilized by π -bonds only. In **7**, the six-membered ring is stabilized by Cs-N bonds, π -interactions and possibly Cs-P contacts, highlighting the importance of a multidentate P,N-coordination sphere in the assembly of this type of a structural motif. The remarkable caesium-“wheel” **7** exhibits a diameter of 2.9 nm in the solid state, which is in the same range as one of the other known hexanuclear Cs-rings.^[43] In case of **7**, the cyclic hexamer forms a central cavity that spans about 7.2 Å between opposing Dipp groups.

Finally, compound **7** was characterized by NMR and IR spectroscopy. In the $^{31}\text{P}\{^1\text{H}\}$ NMR spectrum of **7** a single resonance is detected at $\delta=-20.4$ ppm, hence significantly shifted upfield compared to the former complex $[\text{Cs}\{\text{DPPM}-\text{C}(\text{N-Dipp})_2\}(\text{thf})_x]$ (**6**). In the ^1H NMR and $^{13}\text{C}\{^1\text{H}\}$ NMR spectra the cleavage of a PPh_2 moiety and accompanying formation of a methylene unit is observed ($^{13}\text{C}\{^1\text{H}\}$: $\delta=35.7$ ppm; d , $^1J_{\text{CP}}=13.1$ Hz). Furthermore, another important aspect was to assess whether the six-membered ring structure is also present in solution, since complex **7** exhibits similar luminescence properties in solution and solid state. Therefore, the hydrodynamic radius (r_h) of **7** was determined applying diffusion ordered NMR spectroscopy (DOSY). Here, molecules are distinguished according to their diffusion coefficient (D), which correlates with their hydrodynamic radius.^[45–47] For **7**, a single species with a hydrodynamic radius of $r_h=6.8$ Å (in THF- d_6) is determined in solution

(Supporting Information, Figure S33). In comparison, analogous DOSY measurements of lithium amidinate **1** (in C_6D_6) resulted in a hydrodynamic radius of $r_h = 5.9 \text{ \AA}$ (Supporting Information, Figure S34). Thus, in contrast to the solid state ($r = 14.5 \text{ \AA}$), the DOSY measurements indicate a monomeric species $[Cs-PPh_2CH_2-C(N-Dipp)_2] (1/6 \cdot 7)$ in THF solution. The slightly larger radius compared to **1** is due to the larger ionic radius of caesium, including additional coordinating THF molecules. A measurement of **7** in C_6D_6 was not feasible due to limited solubility. In view of these results, the formation of a hexanuclear ring structure in the solid state seems remarkable, as **7** was crystallized from the strong donor solvent THF, in which it is present in a monomeric form. However, a synthesis by decomposition is not intended to replace a detailed, reproducible procedure for **7**. We believe that the prior synthesis and isolation of the amidine $PPh_2CH_2-C(N-Dipp)_2H$ is the simplest route for the direct formation of caesium complex **7**. The monophosphine amidine is sterically less demanding than DPPM-amidinate **2** and may represent an interesting alternative with respect to the formation of metal complexes.

Photophysical properties

All compounds **1–7** are off-white or colorless crystalline solids. In order to ensure comparability between the alkali metal complexes, only the crystalline, thf-coordinated compounds were used for the measurements. Photoluminescence emission (PL) and excitation (PLE) spectra were recorded for compounds **1–7** in the solid state (Figure 7 and Supporting Information, Figures S42–S48) at temperatures from 6 K to 295 K. Compounds **1–3** and **6** show blue-green photoluminescence at both low (6 or 12 K) and ambient temperature (295 K) with a moderate increase in PL intensity with decreasing temperature (Figure 7). A predominantly blue PL, on the other hand, is observed for potassium compound **4**. In comparison, the PL of rubidium complex **5** is significantly red shifted relative to the other compounds (approx. 50 nm to the protonated ligand **2**), and exhibits green PL at both 6 K and 298 K. The unique caesium ring structure **7** shows a blue-green emission at low temperatures, which is blue shifted upon raising the temperature.

The absorption onset below approximately $\lambda = 450 \text{ nm}$ of the respective spectra of **1–7** is consistent with the colorlessness of the compounds. The emission spectra of the aforementioned compounds, excluding **4**, show fairly broad and unstructured photoluminescence for both low and high temperatures upon UV excitation (below 400 nm). Here, the emission maxima for **1–3** and **6** are centered at approximately $\lambda = 450\text{--}480 \text{ nm}$ (FWHM = 110–165 nm at 295 K, FWHM = full width at half maximum; see Supporting Information, Tables S3 and S4). On the other hand, the hexanuclear Cs-ring **7** features a comparatively sharp emission with a FWHM of 68 nm at 20 K, centered at $\lambda = 393 \text{ nm}$. Interestingly, in comparison to the other alkali metal complexes, potassium compound **4** displays a well resolved vibronic pattern at low temperatures indicating a different relaxation mechanism. The emission band shows two

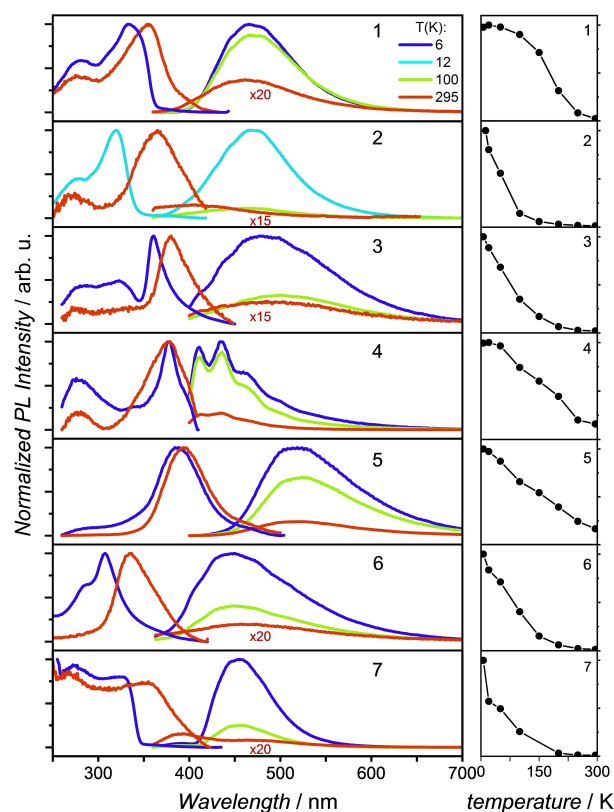


Figure 7. Left: Photoluminescence excitation (PLE) and emission (PL) spectra of compounds **1–7** at 6 (12), 100 and 295 K. Right: Integrated PL intensities plotted against the temperature in the range of 6 to 295 K.

maxima (6 K) at $\lambda_{max} = 411 \text{ nm}$ and 436 nm as well as an additional strong shoulder at 464 nm . Upon raising the temperature from 6 K (respectively 12 K) to 295 K, the PL intensity decreases nearly exponentially for compounds **1–3**, **6** and **7**, while the intensities for the potassium and rubidium complexes **4** and **5** decrease rather linearly (Figure 7, right). In addition, non-radiative electronic relaxation significantly reduces the PL intensity upon raising the temperature, resulting in a low quantum yield of $< 1\%$ (at 295 K) for all compounds except for **4** (see Supporting Information, Table S3). Upon nsec-pulsed laser excitation at 337 nm, the PL of all compounds **1–7** decays within 10 nsec, both at low and ambient temperatures, and therefore can be assigned to fluorescence. No (minor) long-lived phosphorescence component was detected for any of the compounds.

To further compare the specific colors emitted by the compounds **1–7**, we determined the CIE diagrams at 20 K and at 295 K (see Supporting Information, Figures S50 and S51). The diagrams illustrate the azure blue colored PL of $[K\{DPPM-C(N-Dipp)_2\}(thf)_2] (\mathbf{4})$, which is in a distinctly different region compared to the other compounds. For compounds **1**, **3**, **5** and **6** no significant shift of the PL is observed upon temperature decrease, whereas the emission color of **2** is slightly blue shifted upon cooling to cryogenic temperatures.

Conclusion

In conclusion, we present the synthesis of a DPPM-functionalized amidine ligand via a straightforward synthetic protocol. It was feasible to deprotonate the ligand with suitable alkali metal bases to afford the complexes $[M\{\text{DPPM}-\text{C}(\text{N-Dipp})_2\}_n(L)_n]$ ($M = \text{Li}$ (1), Na (3), K (4), Rb (5) Cs (6); $L = \text{thf}$, Et_2O ; $n = 1-3$). In addition, a caesium derivative $[\text{Cs}\{\text{PPh}_2\text{CH}_2-\text{C}(\text{N-Dipp})_2\}_6]$ (7) was obtained as a result of a diphenylphosphino moiety cleavage, forming a remarkable six-membered ring structure in the solid state. Furthermore, PL spectra of all compounds were recorded, showing differences in emission with regards to the respective alkali metal in the blue-green region.

The bifunctional P_2N_2 -design of the ligand, which exhibits orthogonal and opposing functionalities, makes it highly interesting for the construction of advanced metal complexes, allowing various coordination modes. In addition, we envisage that the synthesized amidine/amidates represent a ligand system, which will prove useful for the stabilization of reactive metal species and main group elements, as a result of its high steric demand and multidentate coordination behavior. Future work will emphasize the synthesis of transition metal and lanthanide complexes, as well as the formation of heterometallic structures in view of their potentially interesting photophysical properties.

Experimental Section

The Supporting Information contains experimental details and analytical data of all compounds (NMR, IR, elemental analysis); additional XRD and structure refinement data; NMR- and IR- spectra of every compound; additional PL data. Detailed XRD measurement description as well as crystal and structure refinement data are also provided as Supporting Information. Deposition Number(s) 2091287 (1), 2091288 (2), 2091289 (3), 2091290 (4), 2091291 (5), and 2091292 (7) contain(s) the supplementary crystallographic data for this paper. These data are provided free of charge by the joint Cambridge Crystallographic Data Centre and Fachinformationszentrum Karlsruhe Access Structures service.

Acknowledgements

Financial support by the DFG-funded transregional collaborative research center SFB/TRR 88 "Cooperative Effects in Homo and Heterometallic Complexes (3MET)", projects B3 and C7, is gratefully acknowledged. Open Access funding enabled and organized by Projekt DEAL.

Conflict of Interest

The authors declare no conflict of interest.

Keywords: alkali metals · amidinate · phosphine · photophysical properties · PNNP

- [1] F. T. Edelmann, *Chem. Soc. Rev.* **2009**, *38*, 2253–2268.
- [2] F. T. Edelmann, *Chem. Soc. Rev.* **2012**, *41*, 7657–7672.
- [3] P. Benndorf, J. Jenter, L. Zielke, P. W. Roesky, *Chem. Commun.* **2011**, *47*, 2574–2576.
- [4] P. Benndorf, J. Kratsch, L. Hartenstein, C. M. Preuss, P. W. Roesky, *Chem. Eur. J.* **2012**, *18*, 14454–14463.
- [5] T. S. Brunner, P. Benndorf, M. T. Gamer, N. Knöfel, K. Gugau, P. W. Roesky, *Organometallics* **2016**, *35*, 3474–3487.
- [6] M. P. Coles, D. C. Swenson, R. F. Jordan, V. G. Young, *Organometallics* **1997**, *16*, 5183–5194.
- [7] T. J. Feuerstein, T. P. Seifert, A. P. Jung, R. Müller, S. Lebedkin, M. M. Kappes, P. W. Roesky, *Chem. Eur. J.* **2020**, *26*, 16676–16682.
- [8] S. Fichter, S. Kaufmann, P. Kaden, T. S. Brunner, T. Stumpf, P. W. Roesky, J. März, *Chem. Eur. J.* **2020**, *26*, 8867–8870.
- [9] P. Buchwalter, J. Rosé, P. Braunstein, *Chem. Rev.* **2015**, *115*, 28–126.
- [10] C. Zovko, S. Bestgen, C. Schoo, A. Görner, J. M. Goicoechea, P. W. Roesky, *Chem. Eur. J.* **2020**, *26*, 13191–13202.
- [11] M. P. Coles, P. B. Hitchcock, *Chem. Commun.* **2002**, 2794–2795.
- [12] N. Tsukada, O. Tamura, Y. Inoue, *Organometallics* **2002**, *21*, 2521–2528.
- [13] Z. Feng, Y. Jiang, H. Ruan, Y. Zhao, G. Tan, L. Zhang, X. Wang, *Dalton Trans.* **2019**, *48*, 14975–14978.
- [14] F. Völcker, F. M. Mück, K. D. Vogiatzis, K. Fink, P. W. Roesky, *Chem. Commun.* **2015**, *51*, 11761–11764.
- [15] P. Braunstein, *Chem. Rev.* **2006**, *106*, 134–159.
- [16] C. Fiedel, A. Ghisolfi, P. Braunstein, *Chem. Rev.* **2016**, *116*, 9237–9304.
- [17] R. G. Pearson, *J. Chem. Educ.* **1968**, *45*, 581.
- [18] R. G. Pearson, *J. Chem. Educ.* **1968**, *45*, 643.
- [19] M.-N. Birkholz, Z. Freixa, P. W. N. M. van Leeuwen, *Chem. Soc. Rev.* **2009**, *38*, 1099–1118.
- [20] S. V. Kulangara, C. Mason, M. Juba, Y. Yang, I. Thapa, S. Gambarotta, I. Korobkov, R. Duchateau, *Organometallics* **2012**, *31*, 6438–6449.
- [21] G. Jin, C. Jones, P. C. Junk, A. Stasch, W. D. Woodul, *New J. Chem.* **2008**, *32*, 835–842.
- [22] N. E. Mansfield, M. P. Coles, P. B. Hitchcock, *Dalton Trans.* **2006**, 2052–2054.
- [23] C. Loh, S. Seupel, H. Görls, S. Kriek, M. Westerhausen, *Eur. J. Inorg. Chem.* **2014**, *2014*, 1312–1321.
- [24] M. L. Cole, A. J. Davies, C. Jones, P. C. Junk, *J. Organomet. Chem.* **2004**, *689*, 3093–3107.
- [25] R. A. Burrow, F. C. Wouters, L. Borges de Castro, C. Peppe, *Acta Crystallogr. Sect. E* **2007**, *63*, o2559–o2559.
- [26] D. H. Brown, R. J. Cross, R. Keat, *J. Chem. Soc. Dalton Trans.* **1980**, 871–874.
- [27] T. J. Feuerstein, M. Poß, T. P. Seifert, S. Bestgen, C. Feldmann, P. W. Roesky, *Chem. Commun.* **2017**, *53*, 9012–9015.
- [28] T. Chlupatý, Z. Padělková, A. Lyčka, A. Růžička, *J. Organomet. Chem.* **2011**, *696*, 2346–2354.
- [29] J. Masuda, *Acta Crystallogr. Sect. E* **2008**, *64*, o1447.
- [30] K.-B. Shiu, S.-W. Jean, H.-J. Wang, S.-L. Wang, F.-L. Liao, J.-C. Wang, L.-S. Liou, *Organometallics* **1997**, *16*, 114–119.
- [31] S. Miranda, E. Cerrada, A. Mendía, M. Laguna, *Inorg. Chem. Commun.* **2012**, *21*, 151–154.
- [32] D. J. Elliot, D. G. Holah, A. N. Hughes, H. A. Mirza, E. Zawada, *J. Chem. Soc. Chem. Commun.* **1990**, 32–33.
- [33] J. Ruiz, S. García-Granda, M. R. Díaz, R. Quesada, *Dalton Trans.* **2006**, 4371–4376.
- [34] G. W. Rabe, S. Kheradmandan, L. M. Liable-Sands, I. A. Guzei, A. L. Rheingold, *Angew. Chem.* **1998**, *110*, 1495–1497; *Angew. Chem. Int. Ed.* **1998**, *37*, 1404–1407.
- [35] M. Driess, H. Pritzkow, M. Skipinski, U. Winkler, *Organometallics* **1997**, *16*, 5108–5112.
- [36] G. W. Rabe, H. Heise, G. P. A. Yap, L. M. Liable-Sands, I. A. Guzei, A. L. Rheingold, *Inorg. Chem.* **1998**, *37*, 4235–4245.
- [37] K. Izod, W. Clegg, S. T. Liddle, *Organometallics* **2001**, *20*, 367–369.
- [38] Y. Schulte, C. Stienen, C. Wölper, S. Schulz, *Organometallics* **2019**, *38*, 2381–2390.
- [39] L. Orzechowski, G. Jansen, S. Harder, *Angew. Chem.* **2009**, *121*, 3883–3887; *Angew. Chem. Int. Ed.* **2009**, *48*, 3825–3829.
- [40] A. S. Ionkin, W. J. Marshall, B. M. Fish, A. A. Marchione, L. A. Howe, F. Davidson, C. N. McEwen, *Eur. J. Inorg. Chem.* **2008**, *2008*, 2386–2390.
- [41] T. J. Boyle, L. A. M. Steele, A. M. Saad, M. A. Rodriguez, T. M. Alam, S. K. McIntyre, *Inorg. Chem.* **2011**, *50*, 10363–10370.
- [42] U. Englich, K. Hassler, K. Ruhlandt-Senge, F. Uhlig, *Inorg. Chem.* **1998**, *37*, 3532–3537.

- [43] A. J. Wooles, M. Gregson, S. Robinson, O. J. Cooper, D. P. Mills, W. Lewis, A. J. Blake, S. T. Liddle, *Organometallics* **2011**, *30*, 5326–5337.
- [44] A. J. Veinot, A. D. K. Todd, J. D. Masuda, *Angew. Chem.* **2017**, *129*, 11773–11777; *Angew. Chem. Int. Ed.* **2017**, *1*, 11615–11619.
- [45] R. Neufeld, D. Stalke, *Chem. Sci.* **2015**, *6*, 3354–3364.
- [46] D. Li, I. Keresztes, R. Hopson, P. G. Williard, *Acc. Chem. Res.* **2009**, *42*, 270–280.
- [47] P. Groves, *Polym. Chem.* **2017**, *8*, 6700–6708.

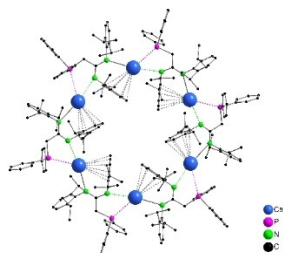
Manuscript received: June 22, 2021

Accepted manuscript online: August 24, 2021

Version of record online: August 24, 2021

FULL PAPER

Combined functionalities: A bis (diphenylphosphino)methane functionalized amidine was synthesized and employed as a ligand for the whole alkali metal series. The resulting complexes show interesting photophysical properties, revealing differences in emission with regards to the respective alkali metal. In addition, a caesium derivative was obtained by cleavage of a diphenylphosphino moiety, forming an unusual six-membered ring structure in the solid state.



*C. Zovko, Dr. C. Schoo, Dr. T. J. Feuerstein, L. Münzfeld, Dr. N. D. Knöfel, Dr. S. Lebedkin, Prof. Dr. M. M. Kappes, Prof. Dr. P. W. Roesky**

1 – 9

Alkali Metal Complexes of a Bis (diphenylphosphino)methane Functionalized Amidinate Ligand: Synthesis and Luminescence



Open Access